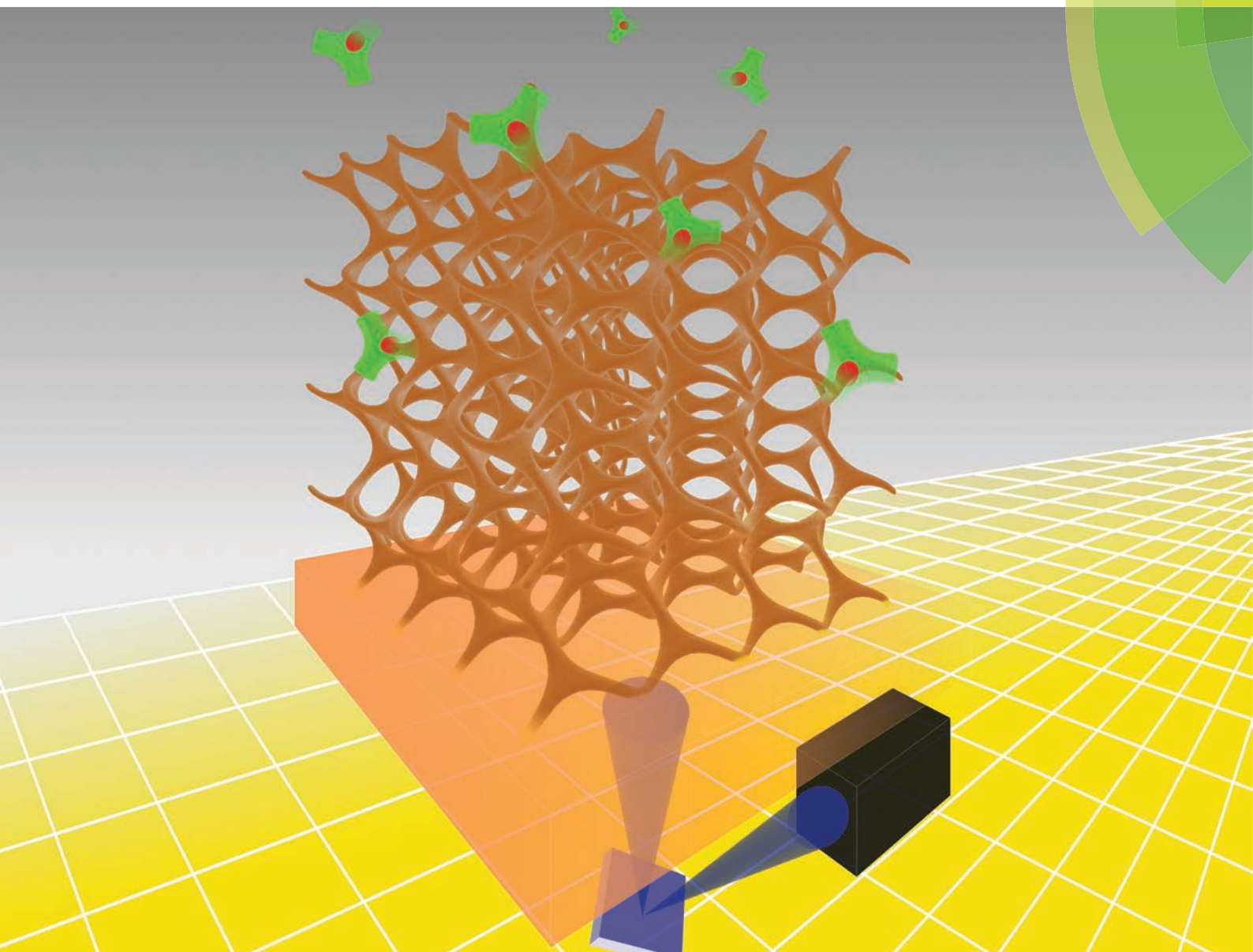


# Biomaterials Science

[www.rsc.org/biomaterialsscience](http://www.rsc.org/biomaterialsscience)



ISSN 2047-4830



## COMMUNICATION

Judith A. Hoyland *et al.*

A microstereolithography resin based on thiol-ene chemistry: towards biocompatible 3D extracellular constructs for tissue engineering



### A microstereolithography resin based on thiol-ene chemistry: towards biocompatible 3D extracellular constructs for tissue engineering†

Cite this: *Biomater. Sci.*, 2014, **2**, 472

Received 13th November 2013,  
Accepted 9th December 2013

DOI: 10.1039/c3bm60290g

www.rsc.org/biomaterialsscience

Ian A. Barker,<sup>a</sup> Matthew P. Ablett,<sup>b</sup> Hamish T. J. Gilbert,<sup>b</sup> Simon J. Leigh,<sup>c</sup> James A. Covington,<sup>c</sup> Judith A. Hoyland,<sup>\*b</sup> Stephen M. Richardson<sup>\*b</sup> and Andrew P. Dove<sup>\*a</sup>

**A new class of degradable aliphatic poly(carbonate) resins for use in microstereolithographic process is described. Using a biologically inert photo-inhibiting dye, exemplar 3-dimensional structures were produced using thiol-ene chemistry via microstereolithography. Fabricated constructs demonstrated good biological compatibility with cells and had tensile properties that render them suitable for use as tissue engineering scaffolds.**

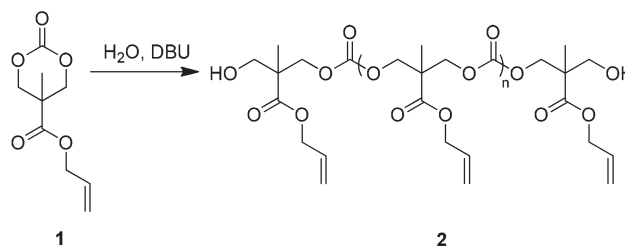
The increasing prevalence of musculoskeletal disorders (MSDs), brought about by an increase in life expectancy and an ageing population, means they are now a leading socio-economic and healthcare burden.<sup>1</sup> However, MSDs affecting cartilaginous tissues, such as osteoarthritis and intervertebral disc (IVD) degeneration, the leading cause of back pain, are difficult to treat. Given the poor long-term outcome of current clinical interventions, research has focussed on the application of cell-based tissue engineering therapies. Autologous chondrocyte re-implantation has demonstrated clinical efficacy for both focal articular cartilage and IVD repair;<sup>2,3</sup> however, for cases where structural integrity of the tissue has been lost, such as in end-stage IVD degeneration, a biomaterial is required to restore tissue volume and mechanical function in the short term, whilst also supporting seeded cells and directing cell function as part of a final medical solution.

A range of natural and synthetic cell-seeded biomaterial scaffolds have been proposed for tissue engineering of cartilaginous tissues, including collagen and silk based natural materials and polymer-based synthetic materials such as PLLA and PCL.<sup>4–7</sup> Importantly, scaffold architecture, including pore

size, porosity and interconnectivity, has been shown to influence cell seeding efficiency and tissue formation. However, in many fabrication methodologies control over these features is process driven, rather than design led. Conversely, additive manufacturing techniques such as 3D bioprinting<sup>8</sup> and microstereolithography<sup>9</sup> ( $\mu$ SL) allow prefabrication of anatomically relevant scaffolds in a layer-by-layer process, that are designed using patient-specific dimensions obtained from MRI or CT scans and subsequent CAD modelling (see ESI†).<sup>10</sup> Such approaches have been shown to support cartilage regeneration *in vivo*<sup>11</sup> and we and others have recently demonstrated the potential of  $\mu$ SL for the generation of 3D cell constructs for tissue engineering.<sup>12–16</sup>

In the current study, using IVD cells as an exemplar system, we have demonstrated the potential of a novel aliphatic poly(carbonate)-based resin for  $\mu$ SL to support cell viability and propose this technology as a mechanism to generate patient-specific prefabricated scaffolds for tissue engineering applications. Most notably, this resin avoids using potentially-toxic acrylate-based crosslinking methodologies, instead focussing on the application of radical based ‘thiol-ene’ chemistries.

An allyl-functional poly(carbonate), **2**, was synthesised by the organocatalytic ring-opening polymerisation (ROP) of the corresponding cyclic carbonate monomer, 5-methyl-5-allyloxy-carbonyl-1,3-dioxan-2-one (MAC, **1**, Scheme 1).<sup>17,18</sup> While typically the strict exclusion of water is desired to produce well-defined polymers by ROP, the ability of water to act as an initiator that, following decarboxylation of the ring-opened



Scheme 1 Synthesis of poly(MAC) by ring-opening polymerisation.

<sup>a</sup>Department of Chemistry, University of Warwick, Coventry, CV4 7AL, UK. E-mail: a.p.dove@warwick.ac.uk; Tel: +44 (0)24 7652 4107

<sup>b</sup>Centre for Tissue Injury and Repair, Institute of Inflammation and Repair, Faculty of Medical and Human Sciences, The University of Manchester, Manchester, M13 9PT, UK. E-mail: Judith.Hoyland@manchester.ac.uk; Tel: +44 (0)161 275 5425

<sup>c</sup>School of Engineering, University of Warwick, Coventry, CV4 7AL, UK

†Electronic supplementary information (ESI) available: Experimental details and additional supporting diagrams and tabulated data. See DOI: 10.1039/c3bm60290g



product, yields a diol that can initiate the synthesis of homo-telechelic polymers (Scheme S1†) enabling the synthesis of polymers with good control over molecular parameters. In this manner, it is possible to produce large quantities of polymers without the requirement to operate in rigorously dry conditions. Analysis of the resulting clear viscous polymer (2) by gel permeation chromatography (GPC) revealed a monomodal molar mass distribution ( $M_n = 5\,870\text{ g mol}^{-1}$  and  $D_M = 1.39$ ; Fig. S2†) with  $^1\text{H NMR}$  spectroscopy (Fig. S3†) revealing that allyl side-chain functionality remained intact after polymerisation and that the average degree of polymerisation (DP), as determined *via* comparison of chain-end methyl units at  $\delta = 1.22\text{ ppm}$  to backbone methyl units at  $\delta = 1.26\text{ ppm}$ , was 10. The control of the quantity of water remaining in the polymerisation solution resulted in the ability to control the molecular weight of the resultant polymers (data not shown).

Utilising thiol–ene click chemistry principles,<sup>19,20</sup> photocrosslinking of 2 was achieved by introducing the four-armed thiol pentaerythritol tetrakis(3-mercaptopropionate) (Fig. S4,† 3) such that the thiol to alkene ratio was 1 : 1. Addition of a titanium based photoradical generator, Irgacure 784 (Fig. S4,† 4), ensured that upon irradiation with light ( $\lambda_{\text{max}} = 465\text{ nm}$ ) cross-linking of the resin occurred in the region of irradiation, solidifying the resin into the desired shape. To apply in  $\mu\text{SL}$ , control over the light penetration depth is required to prevent resin trapped within the 3D structures deleteriously affecting previously cured layers. In turn, this can lead to a number of problems that include increased strain in the fabricated artefact (which can cause the fabricated object to crack) or poor feature fidelity. This problem may be especially pertinent to cross-linked thiol–ene networks since they are known to typically demonstrate high optical clarity.<sup>19,21</sup>

In order to gain control over the cure depth, a photo-inhibitor which absorbs light in the region being employed by the  $\mu\text{SL}$  instrument was added to the mixture. Kalsec Durabrite® Oleoresin Paprika Extract NS (a common food additive), 5, was

selected as a consequence of the high absorbance of the dye in the region of the narrow-band light source being employed in this study (Fig. S5†) and because of the oleophilic nature of the extract. A series of resins were formulated to assess the effect of the paprika extract on cure depth. Polymer 2 was combined with a standard concentration of Irgacure 784 (0.5 wt%), a viscosity modifier (propylene carbonate, 10 wt%) and varying concentrations of the oleoresin dye. A small amount of each formulation was added to a glass microscope slide and subjected to irradiation for 10 s after which, excess uncured resin was washed from the glass slide to leave behind a cured cross-linked film. The thickness of each film was determined using a profilometer (Table S1†). While z-resolution in the 3D fabrication was intended to be carried out at 100  $\mu\text{m}$  layer thicknesses, a slight overcure is required to ensure sufficient bonding of layer-on-layer. As such, a paprika extract (5) concentration of 0.25 wt% was chosen and was found to provide a good level of control over feature fidelity as indicated in the subsequent fabrication of 3D artefacts (see below).

An assessment of the mechanical strength of ‘dogbones’ made from the cured resin was made using standard tensile testing techniques. Typically, the material demonstrated elastic deformation until failure (Fig. S6†) with a Young’s modulus of  $13.1 \pm 0.5\text{ MPa}$ , ultimate tensile strength of  $3.0 \pm 0.1\text{ MPa}$  and elongation at break of  $22.6 \pm 1.0\%$ , in the range required for cartilaginous tissues.<sup>22</sup> The materials demonstrated no plastic deformation and as such no yield point was present during testing, which indicates that failure occurred at microstrain points within the structure.

To assess cell viability and proliferation, suitable constructs produced from the optimised resin were fabricated by impression moulding. In this process, a small quantity of resin (1 drop) was placed on a glass slide and a convex upturned polished circular piece of stainless steel was rested into the centre of the liquid resin. Once the resin had been displaced and with the mould still in place, the glass slide was

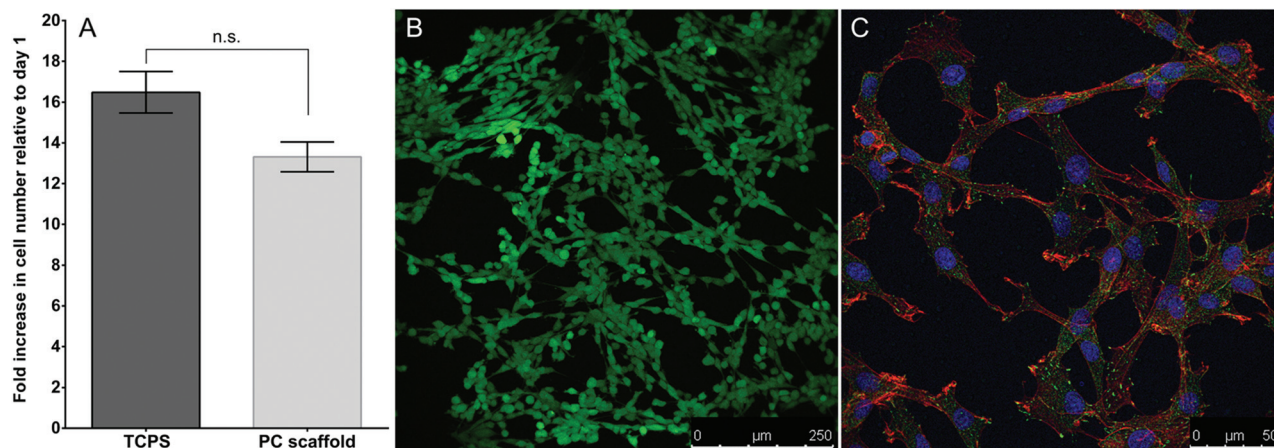


**Fig. 1** Assessment of IVD cell proliferation, viability and morphology on poly(carbonate)-based scaffolds (PC scaffold). IVD cell proliferation was comparable on scaffolds compared to polystyrene tissue culture plates (TCPS) (A;  $n = 3$ , error bars  $\pm$  S.D.) and cells demonstrated high viability (B; green represents viable cells) after 5 days in culture. Adherent IVD cells maintained typical morphology after 7 days in culture (C; red: F-actin, green: vinculin, blue: cell nuclei). n.s. = not significant.





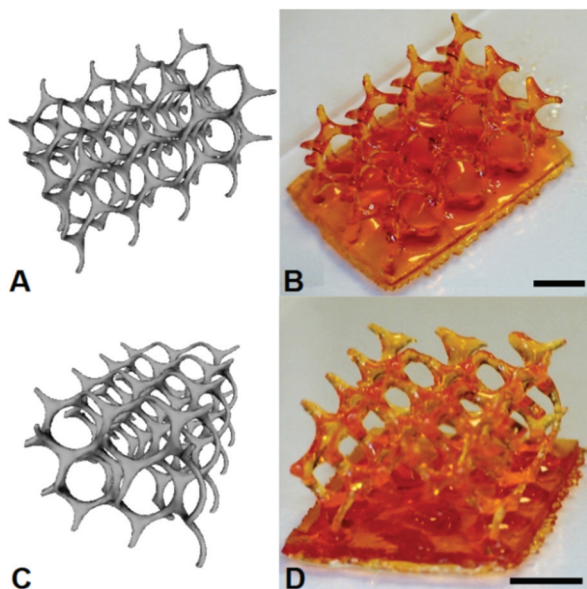


Fig. 2 3D CAD model of the modified (10,3)-a network used in this study (A and C). Fabricated (10,3)-a structure on a 400  $\mu\text{m}$  baseplate to provide a favourable surface to build from and structural integrity (B and D). Scale bars are 2.5 mm.

transferred to an EnvisionTEC Otofash unit and subjected to irradiation (1000 flashes). The metal stub could then be removed from the cured resin to leave behind the construct. Typically, constructs had an 11 mm internal well diameter, to aid in cell containment and a maximum diameter of 14 mm such that they fit in multiwell plates (Fig. S7†).

Proliferation of IVD cells seeded on constructs *versus* polystyrene tissue culture plates (TCPS) was assessed over 5 days (Fig. 1A). IVD cells proliferated both on the polymer constructs and on TCPS over the 5 days, with no significant difference in proliferation between the two culture conditions. IVD cells grown on crosslinked polymer constructs also demonstrated 100% cell viability after 5 days in culture (Fig. 1B) and displayed typical IVD cell morphology (Fig. 1C) after 7 days in culture. Taken together, these data suggest that the cross-linked polymer constructs are non-cytotoxic and equivalent to TCPS for IVD cell growth.

To demonstrate the resin as one that is capable of being used for the fabrication of 3D constructs through  $\mu\text{SL}$ , the production of a (10,3)-a mathematical network was undertaken. Comparison of the 3D CAD structure of the (10,3)-a network with the overall dimensions of  $12.00 \times 8.20 \times 5.50$  mm to the actual fabrication of the structure produced by  $\mu\text{SL}$  resulted in an accurate model devoid of unwanted inclusions with overall dimensions of  $11.50 \times 8.00 \times 5.50$  mm (Fig. 2). As such, the overall shrinkage in the construct was estimated to be approximately 7%.

## Conclusions

In conclusion, crosslinked polymer resins from the aliphatic poly(carbonate), PMAC, and a multi-arm thiol pentaerythritol

tetrakis(3-mercaptopropionate) have been shown to be applicable for 3D-printing (additive layer manufacturing) applications. Furthermore, these materials were shown to support cell proliferation, with such behaviour being comparable on scaffolds produced from these precursors to those in standard monolayer culture with cell viability remaining high over the duration of the study. These results provide a platform for the development of new acrylate-free materials for 3D tissue engineering scaffolds. Further studies are under way to investigate the versatility of these materials for the creation of a range of functional 3D scaffolds.

## Acknowledgements

The Research Councils U.K. (RCUK) are acknowledged for funding a fellowship to S.M.R. We gratefully acknowledge financial support from EPSRC (EP/I014454/1) for funding for I.A.B and BBSRC (BB/I002847/1) for support for H.T.J.G. and M.P.A. The Royal Society is thanked for a Research Grant to facilitate the building of a custom  $\mu\text{SL}$  instrument. The authors also acknowledge George W. Hart for the STL file used for the (10,3)-a structure (retrieved from <http://www.georgehart.com/>).

## Notes and references

- 1 WHO Scientific Group, *The Burden of Musculoskeletal Conditions at the Start of the New Millennium* 919, World Health Organization, Geneva (Switzerland), 2003.
- 2 L. Peterson, M. Brittberg, I. Kiviranta, E. L. Akerlund and A. Lindahl, *Am. J. Sports Med.*, 2002, **30**, 2–12.
- 3 C. Hohaus, T. M. Ganey, Y. Minkus and H. J. Meisel, *Eur. Spine J.*, 2008, **17**, S492–S503.
- 4 M. Sato, M. Kikuchi, M. Ishihara, T. Asazuma, T. Kikuchi, K. Masuoka, H. Hattori and K. Fujikawa, *Med. Biol. Eng. Comput.*, 2003, **41**, 365–371.
- 5 G. Chang, H. J. Kim, D. Kaplan, G. Vunjak-Novakovic and R. A. Kandel, *Eur. Spine J.*, 2007, **16**, 1848–1857.
- 6 H. Mizuno, A. K. Roy, C. A. Vacanti, K. Kojima, M. Ueda and L. J. Bonassar, *Spine*, 2004, **29**, 1290–1297.
- 7 S. M. Richardson, J. M. Curran, R. Chen, A. Vaughan-Thomas, J. A. Hunt, A. J. Freemont and J. A. Hoyland, *Biomaterials*, 2006, **27**, 4069–4078.
- 8 C. H. Lee, J. L. Cook, A. Mendelson, E. K. Moioli, H. Yao and J. J. Mao, *Lancet*, 2010, **376**, 440–448.
- 9 S.-J. Lee, H.-W. Kang, J. K. Park, J.-W. Rhie, S. K. Hahn and D.-W. Cho, *Biomed. Microdevices*, 2008, **10**, 233–241.
- 10 F. P. W. Melchels, J. Feijen and D. W. Grijpma, *Biomaterials*, 2010, **31**, 6121–6130.
- 11 C. H. Lee, J. L. Cook, A. Mendelson, E. K. Moioli, H. Yao and J. J. Mao, *Lancet*, 2010, **376**, 440–448.
- 12 S. J. Leigh, H. T. J. Gilbert, I. A. Barker, J. M. Becker, S. M. Richardson, J. A. Hoyland, J. A. Covington and A. P. Dove, *Biomacromolecules*, 2013, **14**, 186–192.



- 13 J. Jansen, F. P. W. Melchels, D. W. Grijpma and J. Feijen, *Biomacromolecules*, 2008, **10**, 214–220.
- 14 S.-J. Lee, H.-W. Kang, J. Park, J.-W. Rhie, S. Hahn and D.-W. Cho, *Biomed. Microdevices*, 2008, **10**, 233–241.
- 15 F. P. W. Melchels, J. Feijen and D. W. Grijpma, *Biomaterials*, 2009, **30**, 3801–3809.
- 16 I. K. Kwon and T. Matsuda, *Biomaterials*, 2005, **26**, 1675–1684.
- 17 X. L. Hu, X. S. Chen, Z. G. Xie, S. Liu and X. B. Jing, *J. Polym. Sci., Part A: Polym. Chem.*, 2007, **45**, 5518–5528.
- 18 S. Tempelaar, L. Mespouille, P. Dubois and A. P. Dove, *Macromolecules*, 2011, **44**, 2084–2091.
- 19 C. E. Hoyle and C. N. Bowman, *Angew. Chem., Int. Ed.*, 2010, **49**, 1540–1573.
- 20 A. B. Lowe, *Polym. Chem.*, 2010, **1**, 17–36.
- 21 N. B. Cramer, S. K. Reddy, M. Cole, C. Hoyle and C. N. Bowman, *J. Polym. Sci., Part A: Polym. Chem.*, 2004, **42**, 5817–5826.
- 22 S. Yang, K.-F. Leong, Z. Du and C.-K. Chua, *Tissue Eng.*, 2001, **7**, 679–689.

